LARGE AMPLITUDE AERODYNAMIC VIBRATION OF RECTANGULAR CYLINDER WITH A SIDE RATIO OF TWO

Tomomi Yagi[+1], Hisato Matsumiya[+2], Masaaki Hamano[+3], Yuta Sasaki[+4] and Takashi Nishihara[+5]
[+1,3,4]Department of Civil and Earth Resources Engineering, Kyoto University,
Kyoto 615-8540, Japan
[+2,5]Civil Engineering Research Laboratory, Central Research Institute of Electric Power Industry,
Chiba 270-1194, Japan

In general, flutter instabilities of bluff bodies are investigated in the very small amplitude region. The main interests of engineers are to know whether the instabilities appear or not, and to evaluate their onset wind velocities. Therefore, the behaviors of self-induced vibrations at the large amplitude region still remain unexplained. It can be supposed that the amplitudes of so-called divergent type vibrations do not continue increasing all the time, even the structures allow to vibrate. Then, in this study, a rectangular cylinder with a side ratio of two is used to investigate its large amplitude vibrations under three DOF condition with various angles of attack. It is well known that this cylinder shows single DOF flutters, such as the galloping and the torsional flutter at the angle of attack 0 degree. Then, the appearance of aerodynamic interferences between these vibrations is expected in three DOF condition. However, to avoid the interference with Kármán vortices, the wind tunnel tests were conducted at comparatively high reduced wind velocity region. To obtain the large amplitudes in the wind tunnel, the model was mounted by an elastic support system, which is used for the models of overhead transmission lines. Then, the various kinds of self-induced vibration with large amplitudes were observed, e.g. vertical 1DOF dominant vibration, torsional 1DOF dominant vibration, coupled 3DOF vibration and so on. It depends on the angle of attack and the initial condition which phenomenon occurs. To understand these complicated responses, the time history analyses using quasi-steady aerodynamic forces are tried. Also, the aerodynamic force, which has in-phase component to torsional velocity, is added to the quasi-steady formulation virtually. Then, the most of large amplitude vibrations can be explained by using the quasi-steady aerodynamic forces and/or the aerodynamic force attributable to torsional velocity.

Keyword: coupled vibration, galloping, torsional flutter, quasi-steady aerodynamic force

1. INTRODUCTION

Flutter phenomena on bluff bodies can be called as divergent type of aerodynamic vibrations due to rapid increase in amplitude. It is needless to say that the appearance of flutter phenomena on a real structure is not acceptable. Therefore, the specifications of their onset wind velocities or the judgments of their stabilities at the verification wind speed are main targets for the engineering considerations. Then, there are very few investigations on the response behavior of bluff bodies during flutter vibrations. However, due to the recent climate change, the behavior of structures under higher wind velocity than the verification wind speed might be necessary to investigate in future. Furthermore, the large amplitude vibrations of flutter phenomena in 3DOF condition must be also interesting topics on the two dimensional bluff body aerodynamics. Then, in this study, the 3DOF flutter vibrations of a rectangular cylinder are investigated by wind tunnel tests and numerical analyses. For the engineering purposes, the flutter behaviors at around the onset wind velocity and also at very low amplitude region must be of some interest. However, it is not an easy task to make researches in these areas due to existence of strong interference from

[+1]yagi.tomomi.7a@kyoto-u.ac.jp, [+2]hisato-m@criepi.denken.or.jp

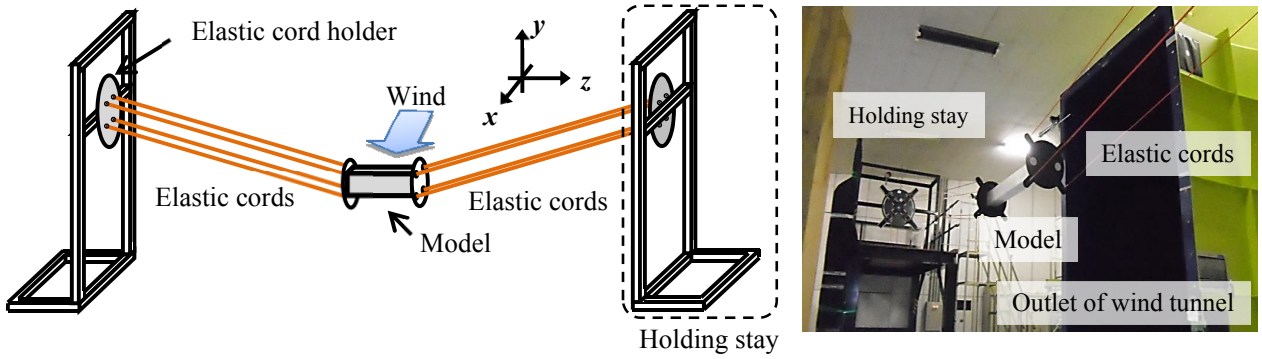

Figure 1: Elastic support system of model in the wind tunnel

vortices shed from the body. To keep the problem simple, the wind tunnel tests were conducted at the comparatively higher reduced wind velocity region and in the larger amplitude region, where the effects of vortex shedding can be avoided.

For a target two dimensional section, a rectangular cylinder with a side ratio two is chosen (B/D=2, where B, D denote width and height of the body, respectively). It is well known that this section shows the galloping instability in the case of vertical 1DOF and torsional flutter in the case of torsional 1DOF. Therefore, it can be expected that the aerodynamic interferences between the galloping and torsional flutter must be appeared in 3DOF conditions. Also, the experiments were conducted by this cylinder with various angles of attack from 0 degree to 90 degree, which means the side ratio of the body varies from 2 to 0.5. In the case of side ratio 0.5, both the galloping and the torsional flutter never appear, but the coupling vibration may happen in 3DOF case. The model was supported in the wind tunnel by using elastic cords, which were developed for the sectional tests of transmission lines to allow large amplitudes[1), 2)]. Then, generation mechanisms of each 3DOF responses from the wind tunnel tests are interpreted by the numerical time series analyses applying quasi-steady aerodynamic forces. The galloping originated responses may be simulated by quasi-steady approach, but the torsional flutter originated responses must be difficult to obtain. The previous researches on the unsteady aerodynamic forces on bluff bodies suggest that the torsional velocity terms must be needed to express the torsional flutter, for example A_2^* in the Scanlan's flutter derivatives[3)]. Therefore, contributions of torsional instabilities in these 3DOF responses are considered by applying additional torsional velocity terms on quasi-steady aerodynamic forces.

2. WIND TUNNEL TESTS

A series of wind tunnel tests were conducted by using an Eiffel-type wind tunnel with an axial fan located in Central Research Institute of Electric Power Industry, Japan. The outlet area of the wind tunnel is 1.6 m width x 2.5 m height, and the maximum wind speed is 17 m/s.

(1) Model

The rectangular cylinder of a side ratio B/D=2 (B: width, D: height) are considered in this study. The size of model for the wind tunnel tests are width B=100mm, height D=50mm and length l=1000mm. The model is made of acrylic resin plates and the circular end plates are installed in the both ends of body.

(2) Supporting system

The model was supported by eight elastic cords as shown in Figure 1. These long elastic cords with low rigidity can obtain the significant large of vibration at law natural frequencies. The system can allow the maximum double amplitudes in the both vertical and horizontal directions till $40D$ and one in the torsional rotation till 180 degree. The natural frequencies in vertical, horizontal, and torsional directions can be controlled by chord length, sag, chord's distance and so on[1)]. Two kinds of structural conditions are considered as follows; the case a) where the vertical and horizontal natural frequencies are set as about 0.5Hz

and the torsional one is set as about 0.9Hz; and the case b) where the all three frequencies are set as about 0.5Hz. In the former case, it is expected that the 1DOF self-induced vibrations such as the galloping or the torsional flutter may easily come out. In the latter case, the 3DOF coupling vibrations must be expected to appear. The wind velocity is fixed as U=10.2m/s and the initial angles of attack are varied from 0 degree to 90 degree. The each case of angles of attack is adjusted at no wind condition, but it will have static displacement under the wind condition and furthermore the equilibrium position (vibration center) will be depends on the amplitude. Therefore, the experimental results are discussed by the equilibrium torsional position of the body, which is referred as a torsional mean displacement Θ_m. The structural parameters are as shown in Table 1. The displacement coordinates x, y, θ denote horizontal direction, vertical direction and torsional direction, respectively. The 3DOF responses were measured by a video tracking system with a frame rate of 60Hz.

Table 1: Structural parameters for free vibration tests.

Case	Equivalent Mass	Equivalent moment of inertia	Wind velocity	Natural frequencies			Reduced wind velocities		
	m [kg]	I [kg·m^2]	U [m/s]	f_x [Hz]	f_y [Hz]	f_θ [Hz]	U/f_xB	U/f_yB	$U/f_\theta B$
a)	3.14	0.0355	10.1	0.47	0.52	0.88	214	195	115
b)	3.14	0.0249	10.2	0.47	0.52	0.50	216	196	205

3. AERODYNAMIC FORCES

(1) Steady aerodynamic coefficients

The steady aerodynamic coefficients defined as follows are also measured for the rectangular cylinder of a side ratio B/D=2 with various angles of attack, as shown in Figure 2.

$$C_D(\alpha)=\frac{Drag}{\frac{1}{2}\rho U^2 Dl},\ C_L(\alpha)=\frac{Lift}{\frac{1}{2}\rho U^2 Bl},\ C_M(\alpha)=\frac{Moment}{\frac{1}{2}\rho U^2 B^2 l} \tag{1}$$

where, C_D, C_L, and C_M are coefficients of drag, lift and pitching-moment, respectively. Also, *Drag*, *Lift*, and *Moment* are the mean values of the measured drag [N], lift [N], and pitching-moment [N·m] on the stationary model and ρ is the air density [kg/m^3]. In Figure 3, Den Hartog's criterion[4)] for the galloping 1DOF instability is plotted. At the angles of attack 0-6 degrees and around 70 degree, Den Hartog criterion shows negative values, where the galloping instability may appears. Also slope of aerodynamic pitching-moment coefficient $dC_M/d\alpha$ is shown in Figure 4 for reference, which might be useful to judge the torsional flutter 1DOF instability. As mentioned above, the torsional flutter 1DOF instability can be explained by the Scanlan's flutter derivative A_2^*, which is the torsional velocity term of unsteady pitching-moment, but may have some relationship to $dC_M/d\alpha$. At the angles of attack 0-10 degrees, $dC_M/d\alpha$ shows negative values, and also from the additional experiments for flutter derivatives, A_2^* shows comparative large positive value (which means large negative damping) at the angle of attack 8 degree. Therefore, the torsional flutter can be generated in this region.

(2) Quasi-steady aerodynamic forces

As shown in Figure 5, the quasi-steady aerodynamic forces can be defined as follows. First of all, the relative wind velocity U_r [m/s] and the relative angle of attack α_r [rad.] can be described as follows. The angle Θ_e denotes the static torsional displacement, and this angle is slightly different from the torsional mean displacement Θ_m, which may be called as the equilibrium positon or the vibration center as mentioned above.

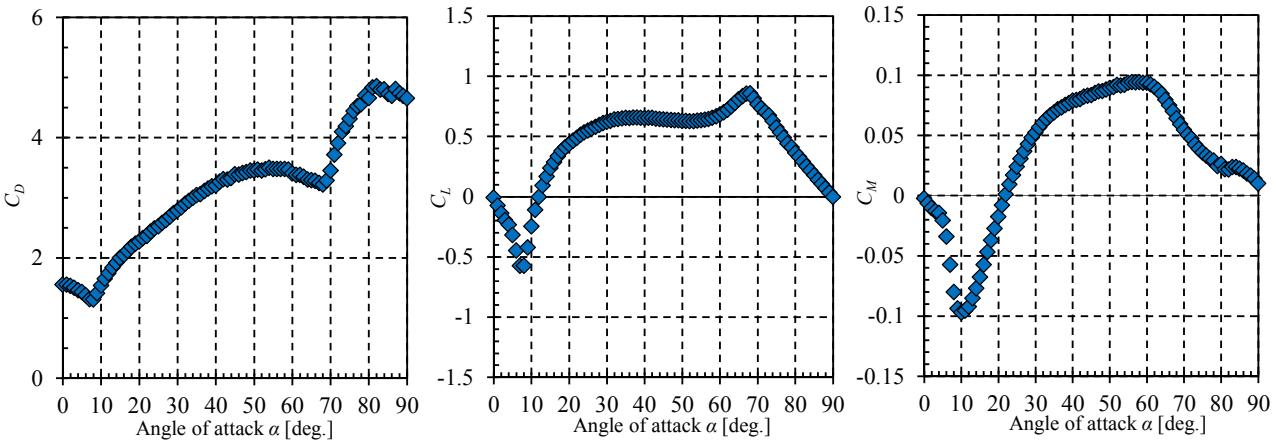

a) Drag coefficient b) Lift coefficient c) Pitching-moment coefficient

Figure 2: Steady aerodynamic coefficients at various angles of attack

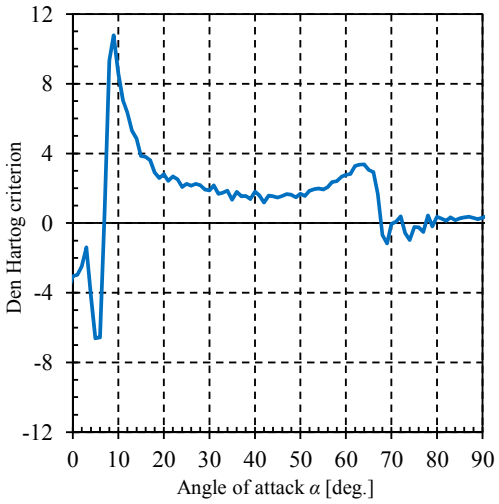

Figure 3: Den Hartog criterion.

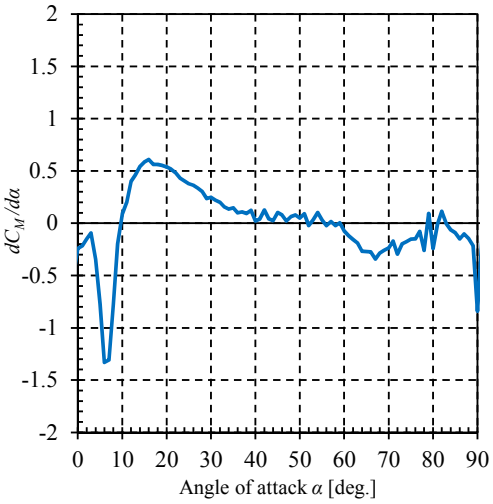

Figure 4: Slope of pitching-moment coefficient.

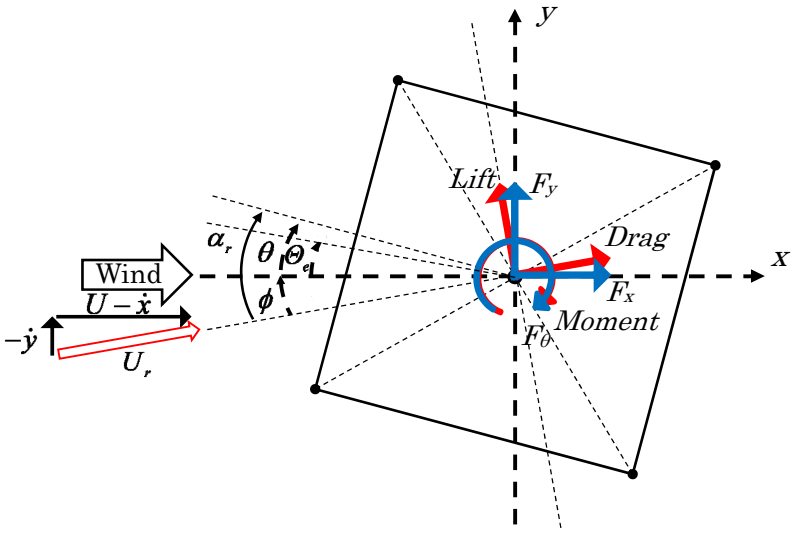

Figure 5: Definition of quasi-steady aerodynamic forces.

$$U_r = \sqrt{(U - \dot{x})^2 + \dot{y}^2} \tag{2}$$

$$\alpha_r = \theta + \phi,\ \phi = \tan^{-1}\left(\frac{-\dot{y}}{U - \dot{x}}\right) \tag{3}$$

Then, the quasi-steady aerodynamic forces in x, y, θ directions as follows.

$$F_x = \frac{1}{2}\rho {U_r}^2 l\{DC_D(\alpha_r)\cos\phi - BC_L(\alpha_r)\sin\phi\} \tag{4}$$

$$F_y = \frac{1}{2}\rho {U_r}^2 l\{DC_D(\alpha_r)\sin\phi + BC_L(\alpha_r)\cos\phi\} \tag{5}$$

$$F_\theta = \frac{1}{2}\rho {U_r}^2 l\left\{B^2 C_M(\alpha_r)\right\} \tag{6}$$

The equations of motions for the body supported by elastic cords in x, y, θ directions are nonlinear equations[1]. Then, substituting the quasi-steady aerodynamic forces of Eqs.(4)-(6) to the equations of motion, the response of the body can be simulated using these governing equations. It is very important to notice that the coupling terms exist in the both structural side and aerodynamic side. However, the coupling vibration due to the structural coupling has no interest. It is quite difficult to eliminate the structural coupling effects from the wind tunnel tests. Therefore, the time series analyses using the non-structural coupling equations must be also needed to discuss this matter.

(3) Additional aerodynamic forces attributable to torsional velocity

In general, to express the instability of 1DOF torsional flutter, the torsional velocity terms of the unsteady aerodynamic pitching-moment must be considered. However, those terms never appears on the quasi-steady formulations. To evaluate the contribution of 1DOF torsional flutter to the 3DOF coupling vibrations, the virtual torsional velocity terms of aerodynamic pitching-moment is added to Eq.(6). Then, virtual aerodynamic pitching-moment can be written as follows.

$$F_\theta = \frac{1}{2}\rho {U_r}^2 B^2 l\left\{C_M(\alpha_r) + 2\pi G\frac{B\dot{\theta}}{U_r}\right\} \tag{7}$$

where the parameter G can control the aerodynamic damping term in Eq.7. If the flutter derivative A_2^* can be assumed to have linear relation with the reduced wind velocity U/fB, then this parameter G is recognized as the slope of A_2^* against the reduced wind velocity U/fB. Of course, the flutter derivative is defined by the unsteady aerodynamic force, and the direct comparison does not have any physical consistency. Furthermore, the effects of this term to the governing equations are almost same as the structural damping in the torsional motion. Then, the values of virtual parameter G are assumed between 0.02-0.20 in this study.

4. AERODYNAMIC VIBRATIONS IN 3DOF

As mentioned above, there are two kinds of combination of natural frequencies for the free vibration tests, which are the case a) $f_x = f_y = 0.5$Hz, $f_\theta = 0.9$Hz and the case b) $f_x = f_y = f_\theta = 0.5$Hz, see Table 1. In the both cases, the vibration amplitudes from the wind tunnel tests and from the time series analyses are compared at each angle of attack, and the vibration mechanisms of these 3DOF phenomena are discussed.

(1) In case of no structural coupling with torsional displacement [case a), $f_x = f_y = 0.5$Hz, $f_\theta = 0.9$Hz]

In this case, the natural frequency of torsional motion is higher than the vertical one and horizontal one. Therefore, the torsional motion and the vertical motion are difficult to couple each other in this system. The results of vibration double amplitudes in 3DOF from the wind tunnel tests and the time series analyses are shown in Figure 6. The lateral axes denote the torsional mean displacement Θ_m. The blue circle plots are

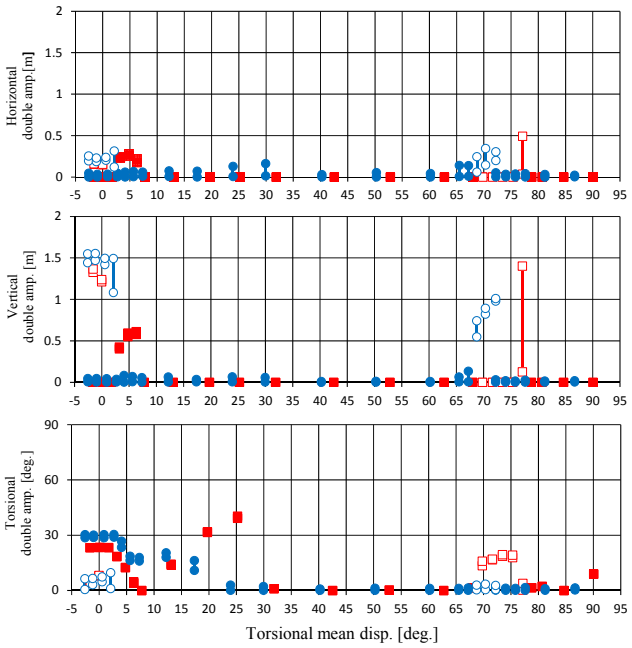

Figure 6: Vibration amplitudes at various torsional mean displacements Θ_m in the case a).
$f_x = f_y = 0.5$Hz, $f_\theta = 0.9$Hz, Experiments (●: mode1, ○: mode2), Analyses (■: mode1, □: mode2)

results from the wind tunnel tests and the red square plots are from the time series analyses. Also, the open plots and solid plots distinguish the different modes, which depend on the initial conditions. Then the around Θ_m=0deg., there are two different modes, one is a large vertical dominant vibration and the other is a large torsional dominant vibration, which never appear in the same time. The blue open circles must be the response due to the galloping at Θ_m= -2 to +2deg. and around 70 deg., which also correspond to negative values of Den Hartog criterion in Figure 3. On the other hands, the blue solid circles must be the torsional flutter at Θ_m= -2 to around 20deg., which corresponds to negative values of $dC_M/d\alpha$ (only at α=0-10 deg.) and also the positive flutter derivative A_2^* till α=20 deg. (from the other additional tests). Around at Θ_m=5deg., the Den Hartog criterion shows negative with comparatively large absolute value, but the galloping never appears in the wind tunnel tests. This might be due to the aerodynamic interferences between the galloping and the torsional flutter.

From the time series analyses using the quasi-steady aerodynamic forces, both of the galloping and the torsional flutter are well simulated around at Θ_m=0deg. It is interesting to see that the galloping in 0.5Hz and the torsional flutter in 0.9Hz exist in the same time at around Θ_m=5deg. The torsional amplitudes tend to decrees against Θ_m more significantly than the data from experiments. Then, if the positive torsional velocity term is included in the aerodynamic pitching-moment, then the torsional response becomes larger, and furthermore the amplitude of the galloping may be reduced by the aerodynamic interferences. Similarly, an opposite case can be seen at around Θ_m=70-75deg. The time series analyses show the torsional response instead of the vertical response. To reduce the torsional responses, the Eq.(7) with negative torsional velocity term G=-0.1 is applied in the governing equations, which means increasing total torsional damping. Then, the torsional responses are vanished and the galloping instabilities appear as same as the experimental results. It can be concluded that the aerodynamic interferences between the galloping and the torsional flutter exist. To simulate this interference precisely, the rational introduction of the torsional velocity term in the aerodynamic pitching-moment must be needed. Furthermore, the appearance of vertical vibration at Θ_m=77deg. is mainly due to the structural coupling terms in equations of motion and the low aerodynamic damping of the torsional motion.

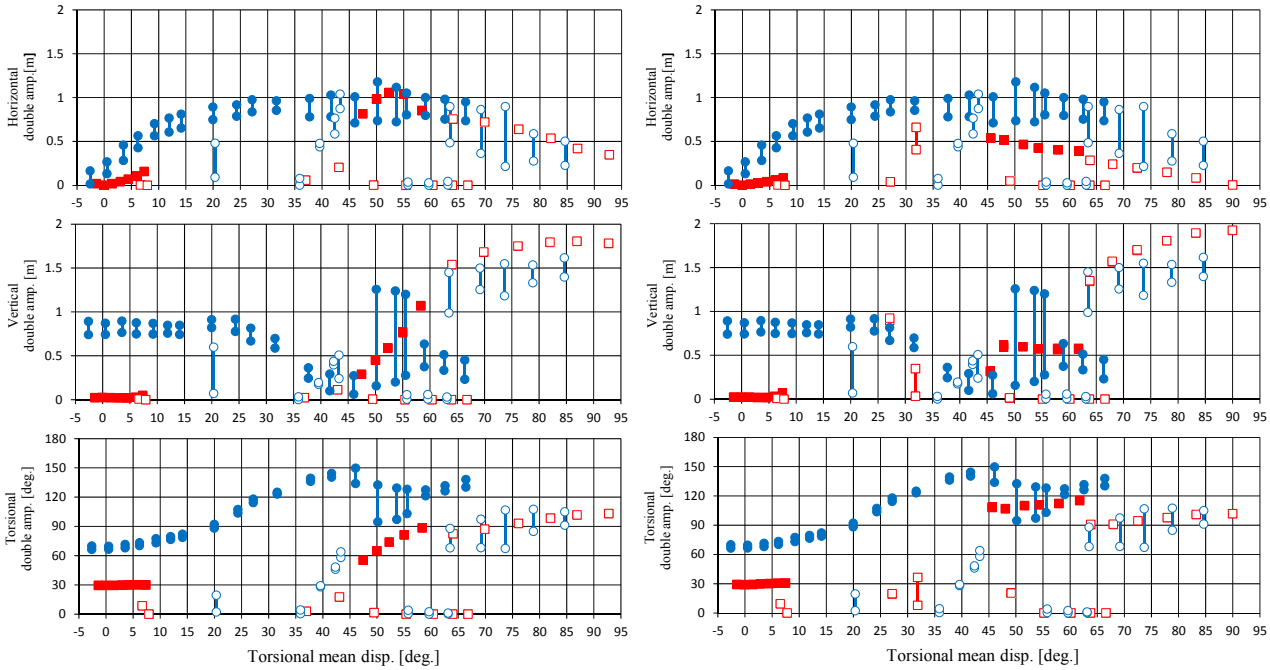

(a) with structural coupling in the analyses (b) without structural coupling in the analyses

Figure 7: Vibration amplitudes at various torsional mean displacements Θ_m in the case b).
$f_x = f_y = f_\theta$=0.5Hz, Experiments (●: mode1, ○: mode2), Analyses (■: mode1, □: mode2)

(2) In case of fully structural coupling in 3DOF [case b), $f_x = f_y = f_\theta$=0.5Hz]

In this case, all of the natural frequencies are almost identical and fully coupling motions in 3DOF are expected. In the same manner as the previous case, the results are shown in Figure 7. To distinguish the 3DOF motions induced by structural coupling or aerodynamically coupling phenomena, the results of time series analyses using the equations of motion without structural coupling terms are also plotted in the Figure 7. Comparing numerical results with the structural coupling and ones without the structural coupling, there are some differences in the amplitudes, but it seems that the 3DOF phenomena due to structural coupling terms are not exist in this case.

From the experimental results, the 3DOF coupled vibration with comparatively large amplitudes are observed through whole range of torsional mean displacement Θ_m. The vibration phenomena can be roughly divided at Θ_m=45deg. Furthermore, in the region Θ_m>45deg., it seems that the response changes from the torsional dominant type to the vertical dominant type around at Θ_m=65deg. Also, the amplitudes of vibrations from the time series analyses coincide well with experimental results at Θ_m>45deg. Therefore, the 3DOF coupling vibrations at Θ_m>45deg. can be explained by quasi-steady aerodynamic forces. However, at Θ_m=-2 to +8deg., the numerical analyses show only the torsional dominant vibrations and their amplitudes are almost half of the experimental results. In this region, the torsional velocity terms in the aerodynamic pitching-moment might be needed. In the region of Θ_m=10-35deg., there is no results from the time series analyses. Even taking into account the static displacements, the vibration center moves to lower angle than Θ_m=10deg.

Then, the torsional velocity term in the aerodynamic pitching moment shown in Eq.(7) is applied in this case. The torsional damping parameter G is determined virtually to keep the torsional amplitude almost same as experimental results, as shown in Figure 8. When the torsional displacements are increased by changing the torsional damping, the 3DOF coupling motion appears and the vertical displacements and horizontal displacements are consistent with those from the wind tunnel tests, especially at Θ_m=0-25deg. Also, the phase differences between vertical motion and the torsional motion agree with experimental results, see Figure 9. Furthermore, introducing the torsional velocity term, the vibration center never moves to the smaller

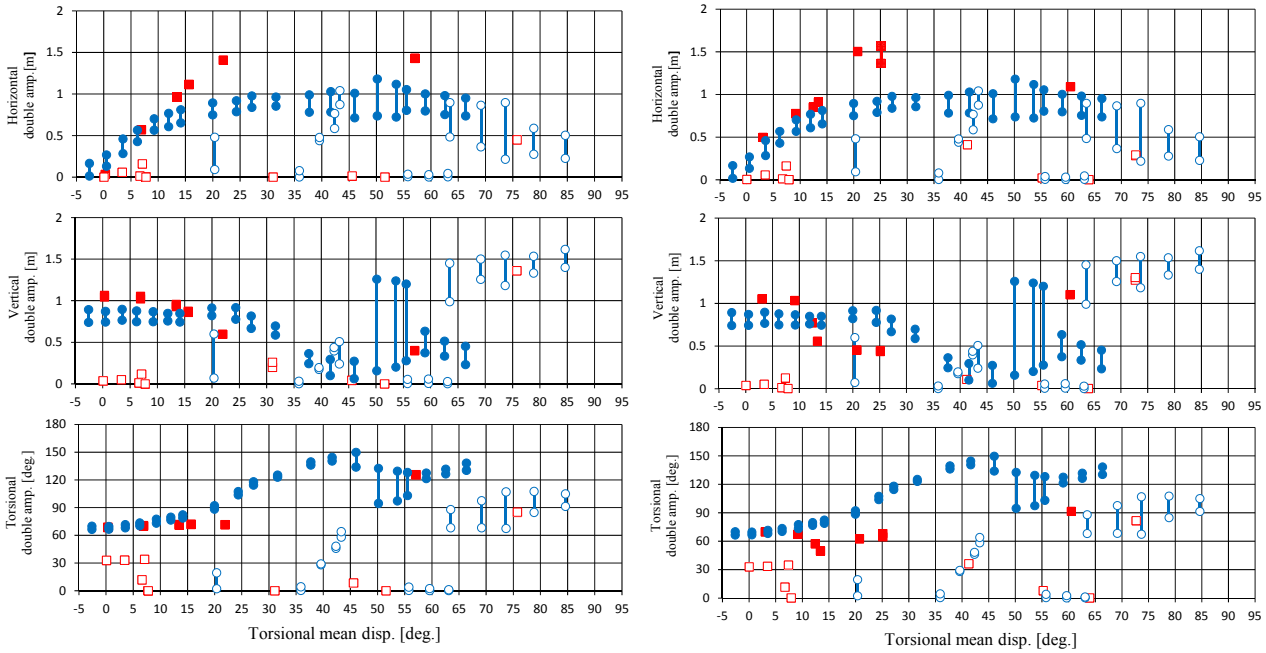

(a) with structural coupling in the analyses (b) without structural coupling in the analyses

Figure 8: Vibration amplitudes at various torsional mean displacements Θ_m in the case b) with additional aerodynamic forces attributable to torsional velocity.
$f_x = f_y = f_\theta$=0.5Hz, Experiments (●: mode1, ○: mode2), Analyses (■: mode1, □: mode2)

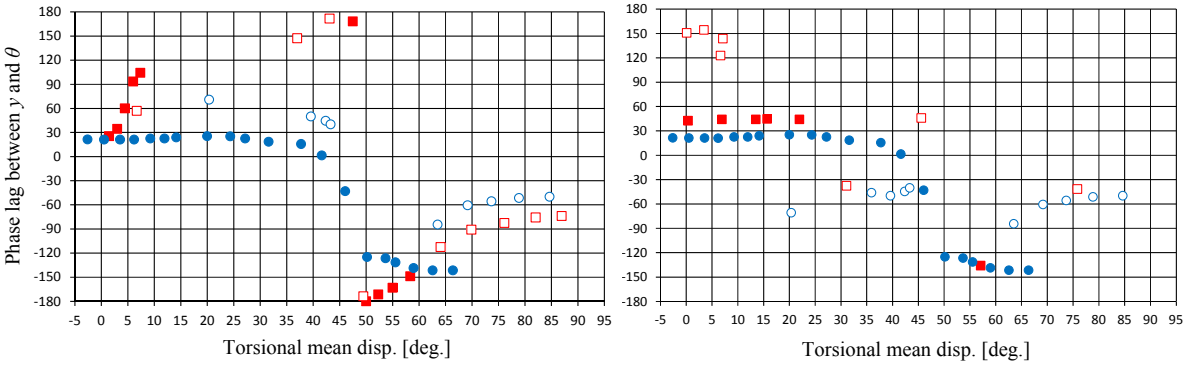

(a) without torsional velocity terms same case as Figure 7(a) (b) with aerodynamic torsional velocity terms same case as Figure 8(a)

Figure 9: Phase lag between vertical displacement and torsional displacement in the case b)
$f_x = f_y = f_\theta$=0.5Hz, Experiments (●: mode1, ○: mode2), Analyses (■: mode1, □: mode2)

angles. Therefore, the 3DOF coupling vibrations in Θ_m=0-25deg. may be torsional flutter initiated instabilities, and to simulate these vibration, the torsional velocity term in the aerodynamic pitching moment must be needed.

4. CONCLUSIONS

The 3DOF large amplitude vibrations are investigated using the rectangular cylinder of a side ratio two with various angles of attack by both of the wind tunnel tests and the time series analyses. Then, the following conclusions are obtained.

1) Both of the 1DOF instabilities such as galloping and torsional flutter with large amplitudes can be simulated by quasi-steady aero dynamic forces in certain extent. However, to discuss the aerodynamic

interference, the additional aerodynamic pitching-moment terms attributable to torsional velocity are needed.

2) 3DOF aerodynamically coupling vibrations at the torsional mean displacements more than Θ_m =45 deg. can be explained by the quasi-steady approach.
3) On the other hand, the aerodynamically coupling vibrations at Θ_m =0-25 deg. must be torsional flutter initiated instabilities, and to simulate these vibration, the torsional velocity terms in the aerodynamic pitching moment are needed.

ACKNOWLEDGMENT

This work was partially supported by the Japan Iron and Steel Federation.

REFERENCES

1) Matsumiya, H., Nishihara, T.: Wind tunnel tests for simulating large-amplitude, low-frequency galloping on overhead transmission lines. *Proc. 7th Colloq. Bluff Body Aerodyn. Appl.*, Shanghai, China, 2012.
2) Matsumiya, H., Nishihara, T.: validation of two quasi-steady aerodynamic force formulations for galloping simulation of four-bundled conductors. *Proc. Symp. Dynamics Aerodyn. Cables*, Copenhagen, Denmark, 2014.
3) Scanlan, R.H., Tomko, J.J. : Airfoil and bridge deck flutter derivatives, *Journal of Engineering Mechanics*, ASCE, Vol.97, No.EM6, pp.1717-1737, 1971.
4) Den Hartog, J.P.: Mechanical Vibrations, *McGraw-Hill*, New York, 1956.